The crystal structure of russellite; a re-determination using neutron powder diffraction of synthetic Bi_2WO_6

KEVIN S. KNIGHT

ISIS Science Division, Rutherford Appleton Laboratory, Chilton, Didcot, Oxon OX12 0QX

Abstract

The crystal structure of the displacive ferroelectric mineral russellite, Bi_2WO_6, has been determined using Rietveld profile refinement of high-resolution, time of flight, neutron powder diffraction data on the synthetic compound. Russellite is orthorhombic, $Pca2_1$, with a 5.43726(2) Å, b 16.43018(5) Å, c 5.458422) Å, $Z = 4$ and is isostructural with the bismuth molybdate mineral koechlinite, Bi_2MoO_6. The structure consists of layers of tilted WO_6 octahedra sandwiched between layers of bismuth and oxygen with the tungsten displaced from the centre of the octahedron by 0.278 Å. The orientations of the lone-pair electrons in the Bi^{3+} cations have been inferred from the 3.0 Å coordination shells of both crystallographically independent bismuths, and have been found to be non-centrosymmetric, an effect which may give rise to the tilting of the WO_6 octahedra. New laboratory source X-ray powder diffraction data are presented for russellite, which, with supplementary synchrotron powder diffractometry, corroborate the new space group and structure determination.

KEYWORDS: russellite, crystal structure, Rietveld analysis, neutron diffraction.

Introduction

THE rare bismuth tungstate mineral russellite was first discovered in the tungsten concentrates at the Castle-an-Dinas mine, St. Columb Major, Cornwall, in 1934 and described as a new species by Hey and Bannister (1938). It has been found subsequently in only three other localities; the Emerald mine, Poona, W. Australia (Hodge, 1970), Bugaya, Uganda (Kagule-Magambo, 1969) and at Corney Fell, west Cumbria, England (Young et al., 1986, 1991). At the Cornish locality, russellite occurs as fine-grained, yellow-green pellets exhibiting a compact texture and an argillaceous odour from fresh surfaces. It is associated with bismuth, bismuthinite, wolf-ramite, limonite, quartz, topaz and schorlite and occasionally encloses gold (Russell, 1944). At Poona, russellite occurs with bismutite, bismite and koechlinite in a small acid pegmatite vein comprising of quartz and muscovite with minor beryl and wolframite. The russellite from west Cumbria occurs as a supergene mineral in an assemblage which includes scheelite, ferberite and chalcopyrite as the major hypogene phases in quartz veins cutting middle Silurian granodiorite.

Although russellite remains a poorly character-ised mineral species, the artificial compound Bi_2WO_6 has been studied in great detail as a result of its exhibiting a number of interesting solid-state and optical properties such as ferroelectricity, piezoelectricity, pyroelectricity and a non-linear dielectric susceptibility (Newkirk et al., 1972; Stefanovich and Venentsev, 1973; Ismailzade and Mirishli, 1970; Yanovskii et al., 1975; Utkin et al., 1980). The author became interested in Bi_2AO_6 type compounds after the discovery of high oxide-ion conductivity in Bi_2UO_6 (Bonanos, 1989) (10^{-1} S cm^{-1} grain interior conductivity at 400 °C), leading to a survey of the structure and transport properties of compounds with analagous stoichiometries. During this work it became apparent that not only was the space group of russellite in doubt but also the crystal system. This paper reports the deter mination of the crystal structure of russellite from high-resolution neutron powder diffraction data carried out on synthetic russellite. The results of the oxide-ion conductivity study of russellite will be published elsewhere.

Experimental

Sample preparation

Synthetic russellite was prepared by solid state reaction of electronic grade purity Bi_2O_3 and WO_3 (Johnson-Matthey Puratronic grade reagents) with the temperature of firing kept well below the principle phase transition temperature of 960 °C (Yanovskii et al., 1975 Wolfe et al., 1969; Watanabe, 1982; Winger et al., 1980; Utkin et al., 1980; Newkirk et al., 1972). Both compounds were weighed to four decimal places, intimately mixed in a gold boat and fired in a muffle furnace under Eurotherm control at 750 °C for 64 hours in air. After the initial firing there was some colour variation evident, from pale yellow-green to yellow, which suggested incomplete reaction. The partially reacted compound was subsequently hand ground, sieved to <40 μm and fired in air at 850 °C for 24 hours. After this second firing, the compound was found to be a uniform pale yellow colour and it was then lightly ground and sieved to <40 μm to produce suitable samples for diffraction analysis.

Powder diffractometry

Neutron time-of-flight diffractometry. Data were collected at room temperature on the high-resolution powder diffractometer (HRPD) (Johnson and David, 1985; David et al., 1988) at the ISIS spallation source, Rutherford Appleton Laboratory. As the spallation source is a pulsed source of neutrons, data are collected at a fixed scattering angle 2θ as a function of the neutron wavelength (Windsor, 1981), with the wavelength being determined by the time-of-flight of the neutron from source to detector. On any time-of-flight diffractometer, the conversion from time-of-flight to d spacing is given by

$$d = ht \operatorname{cosec}(\theta)/(2 \, m_n L)$$

where m_n is the neutron rest mass and L is the total flightpath. The high resolution of HRPD ($\Delta d/d \sim 8 \times 10^{-14}$ over the whole pattern) is achieved by having a long incident flightpath of 95 m, using a neutron guide to avoid flux loss, and by positioning the Li glass scintillator detectors at bakscattering angles of $160° \leq 2\theta \leq 176°$. For this experiment, approximately 50 g of russellite were placed in a 15 mm diameter, cylindrical vanadium can, and data were collected from 30000 μs to 130000 μs, corresponding to an incident wavelength range of $1.2 \text{ Å} \leq \lambda \leq 5.4 \text{ Å}$ and a measured d spacing range of $0.6 \text{ Å} \leq d \leq 2.7 \text{ Å}$. The data collection time corresponded to 319 μAh with ISIS operating at 50 Hz, a circulating proton current of 100 μA and upstream neutron choppers selecting only one pulse in five to prevent frame overlap.

Synchrotron powder diffractometry. Powder diffraction data were recorded using the high-resolution powder diffractometer on station 8.3 at the SERC Synchrotron Radiation Source, Daresbury (SRS) (Cernik et al., 1989). Patterns were collected at a wavelength of 1.0035 Å using dipole radiation from 1.2T bending magnets and monochromated by a 111 silicon, channel-cut, DuMond monochromator (DuMond, 1937; Bonse and Hart, 1965). Wavelength calibration was carried out by least squares fitting of a pseudo-Voight function to the diffraction profiles of three reflections of NBS640b standard silicon powder ($a = 5.430940(3)$ Å). Data collection was carried out with a constant step size of 0.010° and count times of 4 s for $6.00_0 \leq 2\theta \leq 36.00_0$, 6 s for $36.01° \leq 2\theta \leq 56.00°$ and 8s for $56.01° \leq 2\theta \leq 92.00°$. Samples were loaded into standard SRS sample mounts and were rotated at approximately 1 rev. s^{-1} perpendicular to the plane of diffraction. During data collection, the SRS operated at 2 GeV with an average circulating current of 200 mA.

Laboratory source powder diffractometry. The diffractometer sample was prepared by back loading into a sample mount accompanied by automatic agitation and sieving. Minimal pressure was applied from the back of the sample holder to avoid preferred orientation effects which might be expected in a material which exhibits a marked lamellar growth habit (Newkirk et al., 1972; Murumatsu et al., 1978; Payne and Theokritoff, 1975; Voronkova and Yanovskii, 1977). Data were collected in step scan mode using a Siemens D500 diffractometer with Cu-Kα radiation and a post-sample, graphite monochromator. Data collection parameters were from 8.00° 2θ to 88.00° 2θ in 0.04° stes with a 30 s dwell time per step. The incident and diffracted beam collimation was 0.75° and the receiving slit width was 0.018°.

Crystallography

Crystal system

The crystal system of russellite was found to be tetragonal based on a single crystal, grown from a melt of monoclinic $Bi_2(WO_4)_3$ with excess NaCl (Hey and Bannister, 1938). The single crystal rotation photograph was directly superimposable upon the powder pattern of natural russellite and showed the cell to be body-centred with lattice constants $a = 5.42(3)$ Å and $c = 11.3(3)$ Å. Chemical analysis of the artificial compound

showed the formula to be $Bi_2W_2O_9$ significantly different to that determined for the natural mineral. The X-ray diffraction data of Hodge (1970) were subsequently indexed on the cell of Hey and Bannister (op. cit.) although it was not possible to index all the reflections present in the pattern (Hode, op. cit.). Using a limited number of intensity calculations, Hey and Bannister proposed a structure for the cations in russellite with the anion positions determined on geometric grounds.

The Bi_2O_3–WO_3 phase diagram studied by Gal'perin et al. (1966) suggested that Bi_2WO_6 was not in fact tetragonal but orthorhombic with lattice constants $a = 5.436$ Å, $b = 5.456$ Å and $c = 16.416$ Å although the published diffraction data are not of the highest quality. Further work on this system by Hoda and Chang (1974) agreed with the crystal system determination of Gal'perin et al. but no diffraction data were included in their paper. Fig. 1 shows the synchrotron diffraction pattern of our synthetic russellite in the region around the 200 reflection indexed on the cell of Hey and Bannister. The profile shows clearly the power of synchrotron powder diffraction to resolve closely spaced reflections, in this case the 200 apparent singlet reflection into a triplet of 060 002 and 200 (indexed on our cell). There is no evidence in the entire synchrotron pattern of any measurable monoclinic distortion leading to additional line splitting for any of the observed reflections. The presence of many additional reflections in both the synchrotron and laboratory source powder diffraction patterns, that may only be indexed on an orthorhombic cell, are additional proof that the crystal system deduced by Hey and Bannister (op. cit.) is incorrect. Although it is not surprising that Hey

FIG. 1. Synchrotron powder diffraction profiles of the 060, 002 and 200 reflections of synthetic russellite, taken with $\lambda = 1.0035$ Å.
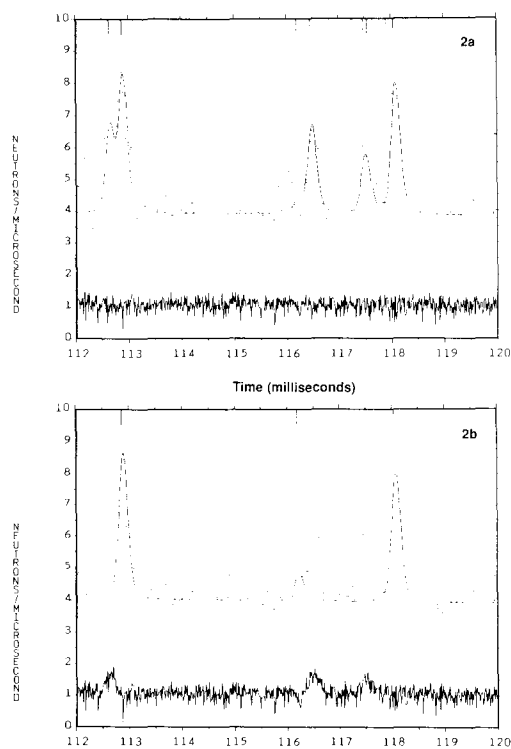
and Bannister were unable to resolve the differences between the a and c axial lengths (our cell) given the limited resolution of their equipment, there is still a major discrepancy between their determination of b and ours.

Space group

Since the work of Hey and Bannister (op. cit.) which suggested possible space groups to be $I\bar{4}2d$ or $I4_1/amd$, there has been widespread disagreement about the true space group of russellite. Gal'perin et al. (1966) found the space group to be $Pccn$, Wolfe et al. (1969) and Newkirk et al. (1972) found $B2cb$, Voronkova and Yanovskii (1977) and Yanovskii et al. (1975) found $Pba2$ and Ismailzade and Mirishli (1970) suggested $Fmm2$ on the basis of it having an Aurivillius phase aristotype. Unpublished X-ray diffraction data determined by Blasse (1966) showed that there was a strong similarity between the diffraction patterns of koechlinite and russellite and Blasse proposed that Bi_2MoO_6 and Bi_2WO_6 were isostructural. The correct space group for koechlinite has also been an area of some controversy (for a discussion see for example Theobald et al., 1984) which has only recently been resolved by Theobald et al. to be $Pca2_1$ using neutron powder diffractometry. Subsequent time-of-flight neutron powder diffraction studies have confirmed the space group as $Pca2_1$ (Teller et al., 1985). The presence of strong second harmonic generation (Stefanovich and Venevtsev, 1973), a large piezoelectric effect and significant pyroelectrical and non-linear optical properties (Yanovskii et al., 1975) shows russellite to have a non-centrosymmetric space group, hence the centrosymmetric space group of Gal'perin et al. may be rejected immediately. In addition, the presence of ferroelectric behaviour shows the correct space group must also be polar. Neither the neutron, synchrotron nor the laboratory source powder data show systematic absences consistent with face-centring and the presence of weak $0kl$ reflections with k odd disprove the possibility of a b glide plane perpendicular to $\mathbf{a}$. We have also determined that the $00l$ systematic absences exist for odd l only and hence space groups $Fmm2$ and $Pba2$ can be rejected. The choice between $B2cb$, $Aba2$ in our orientation, and $Pca2_1$ could only be determined using weak reflections as the structure of russellite we have determined is highly pseudo-symmetric and contains a near A-centring translation. Fig. 2 shows a region of the neutron powder pattern between 112 000 μs and 120 000 μs time-of-flight, fitted using the program CAILS (David et al., 1988) based on the Cambridge Crystallographic

FIG. 2. CAILS refinement of neutron time-of-flight data. Observed (dots), calculated (line) and difference/esd plot (((obs-calc)/esd) + 5)/5)). 2a, Space group $Pca2_1$; 2b, Space group $Aba2$. Abscissa (TOF) in milliseconds.

Subroutine Library (CCSL) (Matthewman *et al.*, 1982, Brown and Matthewman, 1987). The program CAILS allows a structure model-independent, non-linear least squares fitting of Voight functions to diffraction data with peak positions determined by the lattice constants and absences specified by the space group. The refinable variables in the analysis being lattice constants, peak shape parameters and intensities, and the output from the program gives $|F|^2$ for all fitted reflections. In this analysis, neutron data with $105\,000$ μs $\leq$ t $\leq$ $185\,000$ μs was fitted assuming the two alternative space groups $Aba2$ and $Pca2_1$. Fig. 2a shows the fit to space group $Aba2$ (χ^2 for the fitted data $= 1.2$) and Fig. 2b shows the fit to $Pca2_1$ (χ^2 for the fitted data $= 1.1$). The fit to the data is superior in space group $Pca2_1$ especially in the regions where the weak reflections 201, 230 and 112 are evident ($116\,500$ to $118\,500$ μ), these reflections are systematic absences in $Aba2$. Although the evidence of these weak reflections favours space group $Pca2_1$, for confirmation structure refinements were carried out in both

$Aba2$ and $Pca2_1$. High-resolution electron microscopy has shown no evidence for coherent intergrowths of modulated variants in our synthetic russellite (White, pers. comm.) as has been deduced for other Aurivillius type phases.

Structure refinement

Space group $Pca2_1$

The crystal structure was refined from the synchrotron data by the Rietveld method (Rietveld, 1967, 1969) using the program DBW (Wiles and Young, 1981). Starting atomic parameters were those of koechlinite derived from the single crystal analysis of Van Den Elzen and Rieck (1973). Convergence from these trial coordinates was rapid and excellent agreement was found between experimental data and calculated, with agreement factors $R_p = 4.83\%$, $R_{wp} = 6.36\%$ and $R_E = 3.69\%$ for data in the range $26.00°$ $\leq$ 2θ $\leq$ $84.00°$ (for definition of agreement factors see Table 1). However an analysis of bond angles and bond lengths showed a highly distorted octahedral coordination for the tungsten atom and a chemically unreasonable oxygen–tungsten distance of 1.509 Å. It was thought that the atomic number dependence of X-ray scattering was the

Final crystallographic data for russellite at room temperature

Atom	x	y	z	$B_{iso}(Å^2)$
Bi(1)	0.52055(31)	0.42238(10)	0.97608(56)	0.436(29)
Bi(2)	0.48240(31)	0.07712(10)	0.97956(55)	0.595(32)
W	0.00706(78)	0.24948(25)	0.00000*	0.159(22)
O(1)	0.05787(78)	0.14016(28)	0.07680(74)	0.852(77)
O(2)	0.25969(37)	0.99942(21)	0.26347(84)	0.687(87)
O(3)	0.24029(37)	0.50056(20)	0.25763(91)	0.397(74)
O(4)	0.70587(47)	0.23237(14)	0.25069(52)	0.786(34)
O(5)	0.21308(48)	0.26392(16)	0.33079(55)	0.957(37)
O(6)	0.56157(74)	0.35984(27)	0.56183(62)	0.689(80)

* fixed parameter

Orthorhombic: space group $Pca2_1$ (No. 29)

Systematic absences: 0kl, l=2n+1; h0l, h=2n+1.

a=5.43726(20)Å, b=16.43018(50)Å, c=5.45842(20)Å, V=487.63(5)Å^3.

M_r=697.8, ρ_{calc}=9.50gcm^{-3}.

$R_p = \Sigma\,|y_i(obs)\text{-}y_i(calc)|/\Sigma y_i(obs)$ =5.19%.

$R_{wp} = \{\Sigma w_i|y_i(obs)\text{-}y_i(calc)|^2/\Sigma w_i y_i(obs)^2\}^{1/2}$ =5.94%.

$R_E = \{|N\text{-}P+C|/\Sigma w_i y_i(obs)^2\}^{1/2}$ =5.17%.

where N, P and C are the number of observations, parameters and constraints respectively.

probable cause of poor oxygen atom location during the least squares refinement and hence a neutron data set was collected.

The independence of neutron scattering length with atomic number and the small dynamic range of scattering length magnitudes allows the accurate location and refinement of light atoms in the presence of heavy atoms. In the case of russellite, the scattering length used were Bi, 0.8533×10^{-12} cm; W, 0.477×10^{-12} cm and O, 0.5805×10^{-12} cm (Koester et al., 1981). The data from the concentric back scattering detectors were focussed, normalised to the incident monitor spectrum and scaled using a standard vanadium spectrum, giving a range of data $32\,000\ \mu s \le t \le 104\,000\ \mu s$ for profile refinement. The initial structural parameters for the refinement were the coordinates of koechlinite from the neutron powder diffraction study of Theobald et al. (1984). The profile was fitted using a modified Rietveld method, with the peak shape modelled by the convolution of a Voightian (Ahtee et al., 1984; David and Matthewman, 1985) with two decaying exponential functions with different time constants which take into account the effect of the moderator on the neutron energy distribution (David et al. 1988).

In the initial stages of the refinement, the scale factor, the instrumental zero correction, the lattice constants and 5 background parameters (Chebyschev polynomials of the first kind) were all varied, the peak shape parameters were held constant having been initially optimised using a CAILS determination. The two bismuth positional parameters were then refined, followed by the positional parameters of the oxygen atoms and finally the x and y coordinates of the tungsten atom. The peak shape parameters, both the Gaussian and the Lorentzian components, were then optimised and finally the isotropic thermal parameters for all atoms were refined. At this stage of the refinement, all thermal parameters were non-positive definite indicating that an absorption correction to the data was necessary (tungsten has a significant absorption cross section of 18.4×10^{-24} cm^2). After applying the absorption correction to the data, all the temperature factors became positive definite and the refinement converged with $R_p = 5.19\%$, $R_{wp} = 5.94\%$, $R_E = 5.17\%$, $\chi^2 = 1.32$ for 11 786 observations and 48 variables. The thermal parameters of all atoms were less than unity and show only slight variation for the six independent oxygen atoms. The refined structural and isotropic thermal parameters are given in Table 1, and the observed, calculated and difference profiles are shown in Fig. 3. Refinement of extinc-
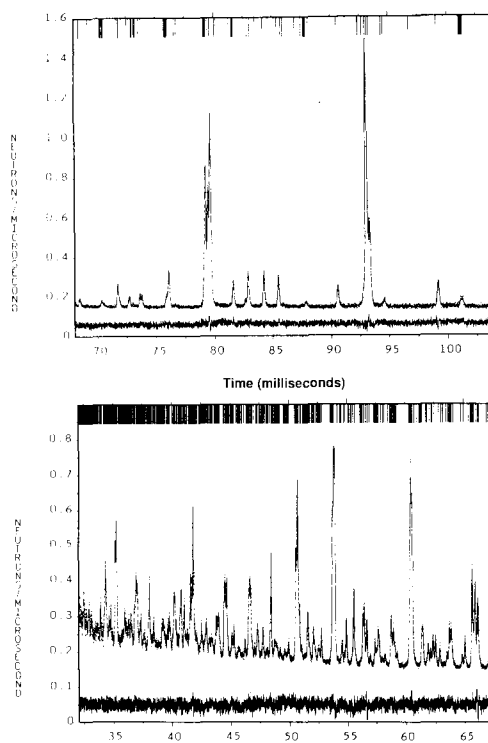

Time (milliseconds)

Fig. 3. Results from the full profile refinement of synthetic russellite. Observed (dots), calculated (line) and difference/esd plot (((obs-calc)/esd) + 5)/100)), observed and calculated profiles offset by 0.1 neutrons/μs. Vertical tick marks indicate the calculated reflection positions for space group $Pca2_1$. Abscissa (TOF) in milliseconds.

tion using the model of Sabine (Sabine, 1985) gave no improvement to the model as measured by the chi-squared of the fit, and site occupancies for all cations remained unity within 1 e.s.d. when refined. Full anisotropic refinement was carried out but led to no significant improvement in the chi-squared of the fit and hence the isotropic model was retained.

Space group Aba2

Wolfe et al. (1969) proposed a structure for russellite in space group $B2cb$ based on a low-resolution neutron powder pattern measured with a wavelength of 1.06 Å in which the orthorhombic distortion was not experimentally observable. The coordinates from this determination were transformed to space group $Aba2$ and used as the starting parameters for profile refinement. Isotropic convergence occurred with $R_p = 7.70\%$, $R_{wp} = 10.28\%$, $R_E = 5.17\%$ and $\chi^2 = 3.94$ for

11 786 observations and 31 variables. The isotropic temperature factors were found to be highly variable with oxygens ranging from 0.8 Å^2 to 3.7 Å^2 and the tungsten atom being non-positive definite even with the application of the absorption correction. Hence, although the number of parameters in space group $Pca2_1$ is larger than those for $Aba2$ the agreement factors and the temperature factors all indicate that the correct space group for russellite is $Pca2_1$.

Description of the structure

The crystal structure of russellite is shown in Fig. 4. The structure can be described as alternating layers of WO_4^{2-} and $Bi_2O_2^{2+}$ lying perpendicular to **b**. The tungstens may be seen to exhibit a moderately regular octahedral environment where neighbouring octahedra are corner sharing whereas the coordination polyhedra of the bismuths is more complex but both are bonded to six oxygens. Bond valence calculations (Brown and Altermatt, 1985) performed for the cations gave

the results W, 6.06; Bi(1), 3.04 and Bi(2), 3.05 in excellent agreement with the expected formal valence of 6 and 3 for tungsten and bismuth respectively. Four types of oxygen can be identified in the structure (Table 2); the first, O(3), is contained entirely within the layers of Bi(1), bridges four cations and has a bond strength of 2.32. O(2) forms the second type and performs a similar role to O(3) in that it is located in the Bi(2) layer and bridges 4 metal atoms. O(2) has a bond strength of 2.34. Oxygen atoms of the third kind, O(4) and O(5), are within the plane of the WO_4^{2-} layers and bridge two tungsten atoms. Calculated bond strengths are 1.87 and 1.94 for O(4) and O(5) respectively. Both of these atoms show weak interactions with the bismuth layers with bond lengths of 3.00 Å for O(5)–Bi(1) and 3.19 Å for O(4)–Bi(2). If these longer range interactions are taken into account the O(4) bond strength increases to 1.90 whilst the bond strength for O(5) becomes 1.99. The final oxygen type, O(1) and O(6), bridges the tungsten and bismuth layers; O(1) is bonded to two Bi(2) atoms and O(6) is bonded to two Bi(1) atoms with bond orders of 1.81 and 1.74 respectively. It is probable that these two oxygen atoms with the lowest coordination number and lowest bond strength are the most easily removed and hence O(1) and O(6) are the most likely candidates for any mobile oxide-ions.

The octahedral environment of the tungsten atom is shown in Fig. 5. The displacement vector of the tungsten atom from the centre of the octahedron is almost entirely in the polar axis direction ($\mathbf{r} = 0.151\mathbf{i} + 0.043\mathbf{j} - 0.986\mathbf{k}$, with $\mathbf{i}, \mathbf{j}, \mathbf{k}$ unit vectors parallel to **a**, **b**, **c** respectively), but the magnitude of the displacement, 0.278 Å, is less than the 0.357 Å determined for koechlinite (Theobald *et al.*, 1984). The displacement vector can be seen to approximately bisect a pseudo 2-fold axis in the WO_6 octahedra and suggests that russellite is a one-dimensional ferroelectric, similar to many oxide perovskites (Lines and Glass, 1977). Theobald *et al.* (op. cit.) have discussed the formation of the koechlinite type structure in terms of tilting of octahedra from an idealised Aurivillius aristotype (Aurivillius, 1952) in a similar manner to the method proposed earlier by Glazer for characterising perovskites (Glazer, 1972). In both cases the maximum angle of tilt of the octahedra is found to be almost identical at 10.3° in russellite and 10.8° in koechlinite (Table 3).

The 3.00 Å coordination spheres of Bi(1) and Bi(2) are nearly identical and are shown in Fig. 6, in which a highly symmetrical oxygen distribution is evident, similar to that observed in koechlinite.
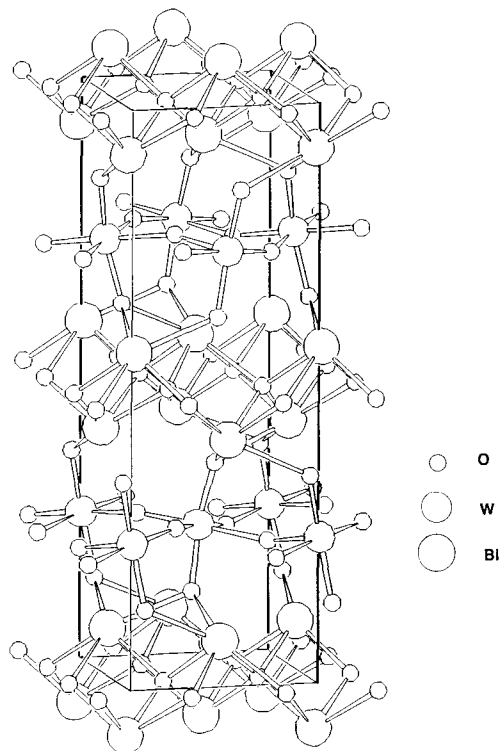
FIG. 4. Crystal structure of russellite, drawn using SCHAKAL88 (Keller, 1988).

O   O
○   W
○   BI

TABLE 2

Selected bond lengths in russellite

Atom 1	Atom 2	Distance(Å)	Atom 1	Atom 2	Distance(Å)	Atom 1	Atom 2	Distance(Å)
Bi(1)	– O(3)	2.517	Bi(2)	– O(1)	2.585	W	– O(1)	1.865
	– O(3)	2.172		– O(1)	2.440		– O(4)	2.152
	– O(3)	2.255		– O(2)	2.345		– O(4)	1.809
	– O(3)	2.322		– O(2)	2.222		– O(5)	2.138
	– O(6)	2.494		– O(2)	2.180		– O(5)	1.796
	– O(6)	2.537		– O(2)	2.501		– O(6)	1.882

Bond strength Bi(1) = 3.04   Bond strength Bi(2) 3.05   Bond strength W = 6.06

Closest oxygen–oxygen distance O(1) – O(5) 2.602 Å
Estimated standard deviations on all bond lengths 0.005 Å

FIG. 5. WO$_6$ octahedron showing the displacement of the tungsten atom away from the centre of the octahedron in the polar axis direction.

The electronic configuration of Bi^{3+} is [Xe]4f^{14}5d^{10}6s^2 and Teller *et al.* have suggested that the asymmetry of the oxygen disposition in koechlinite is related to the location of the lone-pair electrons (Teller *et al.*, 1984). Assuming the lone-pair position is 'beneath' the oxygen coordination hemisphere, then Fig. 3 shows that all bismuth atoms direct their lone-pairs into the tungsten layers and hence each WO$_6$ octahedra is influenced by the surrounding two bismuth layers. In addition, the lone pairs in the two layers are not related in a centrosymmetric manner and thus it is tempting to speculate that the tilting of the octahedron may be related to this lone-pair asymmetry.

TABLE 3

Selected bond angles in russellite

At1	At2	At3	Angle (Degrees)
O(1)	- W-	O(4)	81.0, 96.6
O(1)	- W-	O(5)	80.8, 96.7
O(1)	- W-	O(6)	156.5
O(4)	- W-	O(4)	88.3
O(4)	- W-	O(5)	82.9, 171.4, 100.1, 171.1
O(4)	- W-	O(6)	82.0, 99.1
O(5)	- W-	O(5)	88.6
O(5)	- W-	O(6)	81.1, 97.6

At1	At2	At3	Angle (Degrees)
O(3) -	Bi(1)	- O(3)	69.6, 68.2, 75.8, 74.8
O(3) -	Bi(1)	- O(6)	71.9, 78.6, 79.1, 68.8
O(6) -	Bi(1)	- O(6)	85.4
O(1) -	Bi(2)	- O(1)	86.3
O(1) -	Bi(2)	- O(2)	67.7, 78.8, 79.5, 73.0
O(2) -	Bi(2)	- O(2)	74.1, 68.2, 76.3, 70.4

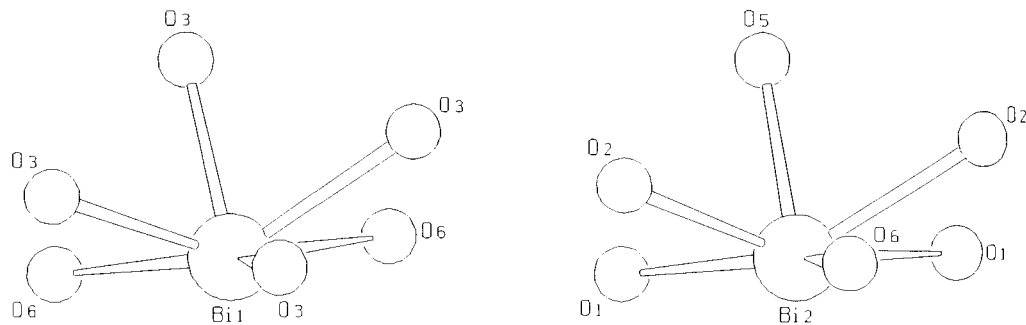Estimated standard deviations on all bond angles 0.2°

TABLE 4

X-ray powder diffraction data for russellite

h	k	l	d (Å)	Intensity
0	2	0	8.22	2
1	2	0	4.53	1
0	4	0	4.11	1
1	1	1	3.75	1
1	4	0	3.277	1
1	3	1	3.151	100
0	6	0	2.738	29
0	0	2	2.729	22
2	0	0	2.719	22
0	2	2	2.590	<1
2	2	0	2.581	<1
1	5	1	2.500	3
2	1	1	2.407	1
1	2	2	2.338	1
2	4	0	2.267	<1
1	7	1	2.004	1
2	5	1	1.956	1
0	6	2	1.933	16
2	6	0	1.929	10
2	0	2	1.926	19
2	2	2	1.875	1
3	2	0	1.770	1
2	4	2	1.744	1
1	1	3	1.716	1
2	5	2	1.662	<1
3	4	0	1.658	1
1	9	1	1.650	20
1	3	3	1.646	21
0	10	0	1.643	10
2	8	0	1.639	2
2	6	2	1.575	21
1	5	3	1.528	1
2	1	3	1.506	<1
3	2	2	1.485	1
3	4	2	1.417	1
0	10	2	1.408	1
2	10	0	1.406	1
2	8	2	1.405	1
1	11	1	1.393	1
1	7	3	1.390	1
3	7	1	1.387	<1
0	12	0	1.369	4
0	0	4	1.364	3
0	2	4	1.346	<1
4	1	1	1.315	1
2	7	3	1.271	<1
1	9	3	1.254	9
3	9	1	1.252	9
1	13	0	1.231	<1
2	12	0	1.223	2
0	6	4	1.221	7
2	0	4	1.219	6
2	2	4	1.206	<1
1	13	1	1.201	1
4	7	1	1.150	1
1	11	3	1.129	1
3	11	1	1.128	1
2	12	2	1.116	6
2	6	4	1.114	7

Chang and it is possible that at this locality, the material analysed may be a mixture of russellite with a possibly new bismuth-rich tungsten oxide mineral. The phase diagram of Hoda and Chang show that the composition Bi_4WO_9 is a mixture of the phases Bi_2WO_6 and $Bi_{14}W_2O_{27}$ in the ratio 3 : 1; however Young *et al.* state that their material shows significant line broadening and hence it would not be an easy task to prove whether this russellite was in fact a two-phase mixture or single phase although detailed X-ray line-profile analysis may yield some useful information. Chemical variability of the Cornish material was also noted by Hey and Bannister (op. cit.), who in addition, found that the X-ray diffraction pattern of green pellets from Castle-an-Dinas was quite distinct from russellite. Unfortunately no published data exist for the X-ray powder diffraction pattern for the green pellets and hence its relationship to the other possible polymorphs of Bi_2WO_6 is unknown.

The observed densities measured by Hey and Bannister are more difficult to reconcile in that they were so low for compounds of these compositions that it led Blasse (1966) to propose that their structures were clearly incorrect. However the natural texture of the Cornish and the Cumbrian mineral precludes easy density determination and it is quite possible that some of the NaCl flux was included in the single crystal leading to the anomalously low observed density.

Solid state physics

The physical properties of Bi_2WO_6 are of great interest for possible solid-state device applications such as frequency doublers or oscillators. However, from the measured tungsten displacement it is apparent that russellite is not a conventional ferroelectric and does not obey the Abrahams-Kurtz-Jamieson relationship for displacive ferroelectrics on the assumption that the hexavalent element is acting as the homopolar cation (Abrahams *et al.*, 1968). The predicted ferroelectric–paraelectric phase transition temperature, T_c, based on the AKJ relationship, is 1546 K for russellite far in excess of the melting point of 1433 K (Newkirk *et al.*, 1972). Several phase transitions have been proposed in russellite on the basis of DTA and temperature dependent dielectric susceptibility measurements, although both the temperatures at which they occur and whether they represent a ferroelectric-paraelectric transitions are in dispute (Utkin *et al.*, 1980; Watanabe, 1982; Winger *et al.*, 1980; Yanovskii *et al.*, 1974). The principal phase transition for which there appears to be no disagreement occurs

at ~1233 K and is first-order and reconstructive possibly to a phase isostructural with $BiLaWO_6$ (Watanabe, 1982). Maxima in both the dielectric constant and the dielectric loss tangent have been observed in the temperature range 673 K to 1000 K by Utkin *et al.*, although they do not appear to relate to the ferroelectric–paraelectric transition as second harmonic generation maximises in this temperature range and has been observed at temperatures up to the first-order transition (Stefanovich and Venetseev, 1973). It is possible that this additional transition is a subtle displacive phase transition between one non-centrosymmetric space group to another, mediated by rigid unit modes. If this were so, it would not necessarily require the tungsten displacement vector within the octahedra to tend to zero at the transition temperature resulting in russellite becoming paraelectric. Unfortunately there has been no Raman spectroscopy carried out on Bi_2WO_6 as a function of temperature and hence the presence of rigid unit modes remains purely speculative. The crystallography of Bi_2WO_6 as a function of temperature is currently being carried out using neutron powder diffraction to attempt to resolve some of these ambiguities.

Conclusions

The crystal structure of russellite has been refined to high accuracy on a synthetic sample of Bi_2WO_6 using the Rietveld method with high-resolution, time-of-flight, neutron powder diffraction data. The results disprove not only the space group but also the crystal system determined by Hey and Bannister (1938) from X-ray studies of the natural mineral and an artificial flux-grown single crystal. Russellite has been found to be orthorhombic, space group $Pca2_1$ with near integral axial ratios. The crystal structure determined shows russellite to be a bismuth tunstate not a disordered mixed-oxide phase as had been inferred by Hey and Bannister. Bond valence calculations carried out on the cations is in excellent agreement with formal valencies. The coordination of the two crystallographically distinct bismuth ions are close to being identical, and the lone-pair orientation for both ions has been inferred from the 3.0 Å oxygen coordination shells. The tungsten is six-fold coordinated but displaced from the centre of a regular octahedra giving rise to ferroelectric behaviour. Simulation of laboratory-source X-ray pmwder diffraction patterns with a significant line-broadening contribution is in good agreement with the data of Hodge (1970) for the natural mineral from Poona.

References

Abrahams, S. C., Kurtz, S. K., and Jamieson, P. B. (1968) Atomic displacement relationship to Curie temperature and spontaneous polarisation in displacive ferroelectrics. *Phys. Rev.*, **172**, 551-3.

Aurivillius, B. (1952) The structure of Bi_2NbO_5F and isomorphous compounds. *Arkiv fur Kemi*, **5**, 39-47.

Ahtee, M., Unonius, L., Nurmela, M., and Suortti, P. (1984) A Voightian as profile shape function in Rietveld refinement. *J. Appl. Crystallogr.*, **17**, 352-7.

Blasse, G. (1966) Polymorphism of Bi_2MoO_6. *J. Inorg. Nucl. Chem.*, **28**, 1124-5.

Bonanos, N. (1989) High oxide ion conductivity in bismuth uranate, Bi_2UO_6. *Mat. Res. Bull.*, **24**, 1531-40.

Bonse, U. and Hart, M. (1965) Tailless X-ray single-crystal reflection curves obtained by multiple reflection. *Appl Phys Letters*, **7**, 238-40.

Brown, I. D. and Altermatt, D. (1985) Bond-valence parameters obtained from a systematic analysis of the inorganic crystal structure database. *Acta Cryst.*, **B41**, 244-7.

Brown, P. J. and Matthewman, J. C. (1987) The Cambridge crystallography subroutine library—mark 3 user's manual. Rutherford Appleton Laboratory Report, RAL-87-010.

Cernik, R. J., Murray, P. K., Pattison, P., and Fitch, A. N. (1989) A two circle powder diffractometer for synchrotron radiation with closed loop encoder system. Daresbury Preprint DL/SCI/P669E.

David, W. I. F. and Matthewman, J. C. (1985) Profile refinement of powder diffraction patterns using the Voight function. *J. Appl. Crystallogr.*, **18**, 461-6.

—— Akporiaye, D. E., Ibberson, R. M., and Wilson, C. C. (1988) The high resolution powder diffractometer at ISIS—an introductory users guide. Rutherford Appleton Laboratory Report.

DuMond, J. W. M. (1937) Theory of the use of more than two successive X-ray reflections to obtain increased resolving power. *Phys. Rev.*, **52**, 872-83.

Gal'perin, E. L., Erman, Y. Ya., Kolchin, I. K.,

Belova, M. A., and Chernyshev, K. S. (1966) X-ray diffraction examination of the Bi_2O_3–WO_3 system. *Zh. Neorgan. Khim.*, **11**, 1125–30.

Glazer, A. M. (1972) The classification of tilted octahedra in perovskites. *Acta Cryst.*, **B28**, 3384–92.

Hey, M. H. and Bannister, F. A. (1938) Russellite, a new British mineral. *Mineral. Mag.*, **25**, 41–55.

Hoda, S. N. and Chang, L. L. Y. (1974) Phase relations in the system Bi_2O_3–WO_3. *J. Amer. Ceram. Soc.*, **57**, 323–6.

Hodge, L. C. (1970) Russellite: second occurrence. *Mineral. Mag.*, **37**, 705–7.

Ismailzade, I. G., Mirishli, F. A. (1970) High-temperature X-ray and dielectric investigation of Bi_2WO_6. *Kristallografiya*, **14**, 738–9.

Johnson, M. W. and David, W. I. F. (1985) HRPD: The high resolution powder diffractometer at the SNS. Rutherford Appleton Laboratory Report RAL-85-112.

Kagule-Magambo, J. (1969) Ann. Rept. Geol. Surv. and Mines Dept. Uganda, 6–8. [M.A. 72–1015.]

Keller, E. (1989) Some computer drawings of molecular and solid-state structures. *J. Appl. Crystallogr.*, **22**, 19–22.

Koester, L., Rauch, H., Herkens, K., and Schroder, K. (1981) Summary of neutron scattering lengths, K.F.A. Report, Jul-1755.

Lines, M. E. and Glass, A. M. (1977) *Principles and applications of ferroelectrics and related materials.* Clarendon Press, Oxford.

Matthewman, J. C., Thompson, P. , and Brown, P. J. (1982) The Cambridge crystallography subroutine library. *J. Appl. Crystallogr.*, **15**, 167–73.

Murumatsu, K., Watanabe, A., and Goto, M. (1978) Flux growth of Bi_2WO_6 below the phase transition temperature. *J. Crystal Growth*, **44**, 50–2.

Newkirk, H. W., Quadflieg, P., Liebertz, J., and Kockel, A. (1972) Growth, crystallography and dielectric properties of Bi_2WO_6. *Ferroelectrics*, **4**, 51–5.

Payne, D. A. and Theokritoff, S. (1975) Hydrothermal recrystallisation of Bi_2WO_6. *Mat. Res. Bull.*, **10**, 437–42.

Rietveld, H. M. (1967) Line profiles of neutron powder-diffraction peaks for structure refinement. *Acta Cryst.*, **22**, 151–2.

—— (1969) A profile refinement method for nuclear and magnetic structures. *J. Appl. Crystallogr.*, **2**, 65–71.

Russell, A. (1944) Some minerals new or rare to Britain. *Mineral. Mag.*, **27**, 1–10.

Sabine, T. M. (1985) Extinction in polycrystalline materials. *Aust. J. Phys.*, **38**, 507–18.

Stefanovich, S. Yu. and Venetsev, Yu. N. (1973) Definition of some parameters of ferroelectric crystals by the SHG method. *Phys. Stat. Sol.(a)*, **20**, K49–52.

Theobald, F., Laarif, A. and Hewat, A. W. (1984) The structure of koechlinite bismuth molybdate—a controversy resolved by neutron diffraction. *Ferroelectrics*, **56**, 219–37.

Teller, R. G., Brazdil, J. F., Grasselli, R. K., and Jorgensen, J. D. (1984) The structure of γ bismuth molybdate, Bi_2MoO_6, by powder neutron diffraction. *Acta Crystl.*, **C40**, 2001–5.

Utkin, V. I., Roginskaya, Yu, E., Voronkova, V. I., Yanovskii, V. K., Galyamov, B. Sh., and Venetsev, Yu. N. (1980) Dielectric properties, electrical conductivity and relaxation phenomena in ferroelectric Bi_2WO_6. *Phys. Stat. Sol.(a)*, **59**, 75–82.

Van Den Elzen, A. F. and Rieck, G. D. (1973) Redetermination of the structure of Bi_2MoO_6, Koechlinite. *Acta Cryst.* **B29**, 2436–8.

Voronkova, V. I. and Yanovskii, V. K. (1977) Growth of Bi_2WO_6 crystals. *Kristallografiya*, **22**, 429–30.

Watanabe, A. (1982) Polymorphism in Bi_2WO_6. *J. Solid State Chemistry*, **41**, 160–5.

Wiles, D. B. and Young, R. A. (1981) A new computer program for the analysis of X-ray powder diffraction patterns. *J. Appl. Crystallgor.*, **14**, 149–51.

Windsor, C. G. (1981) *Pulsed neutron scattering.* Taylor and Francis, London.

Winger, L. A., Bradt, R. C., and Hoke, J. H. (1980) Transformational superplasticity of Bi_2WO_6 and Bi_2MoO_6. *J. Amer. Ceramic Soc.*, **63**, 291–4.

Wolfe, R. W., Newnahm, R. E., and Kay, M. I. (1969) Crystal structure of Bi_2WO_6. *Solid State Comm.*, **7**, 1797–801.

Yanovskii, V. K., Voronkova, V. I., Alexandrovskii, A. L., and D'yakov, V. A. (1975) Structure and properties of Bi_2WO_6 ferroelectric crystals. *Dokl. Akad. Nauk SSSR*, **222**, 94–5.

Young, B., Fortey, N. J., and Nancarrow, P. H. A. (1986) An occurrence of tungsten mineralisation in the Eskdale intrusion, west Cumbria. *Proc. Yorkshire Geol. Soc.*, **46**, 15–21.

—— —— —— (1991) Russellite from Buckbarrow Beck, Cumbria, England. *J. Russell Society*, **4**, 3–7.